THE GEOLOGICAL SOCIETY OF AMERICA®

CO_2 diffusion into pore spaces limits weathering rate of an experimental basalt landscape

Joost van Haren[1]*, Katerina Dontsova[1], Greg A. Barron-Gafford[1,2], Peter A. Troch[1,3], Jon Chorover[1,4], Stephen B. Delong[1,5], David D. Breshears[1,6,7], Travis E. Huxman[1,8], Jon D. Pelletier[1,9], Scott R. Saleska[1,7], Xubin Zeng[1,10], and Joaquin Ruiz[1,9,11]

[1]Biosphere 2, University of Arizona, Tucson, Arizona 85721, USA
[2]School of Geography and Development, University of Arizona, Tucson, Arizona 85721, USA
[3]Department of Hydrology and Water Resources, University of Arizona, Tucson, Arizona 85721, USA
[4]Department of Soil, Water and Environmental Science, University of Arizona, Tucson, Arizona 85721, USA
[5]U.S. Geological Survey, Menlo Park, California 94025, USA
[6]School of Natural Resources and the Environment, University of Arizona, Tucson, Arizona 85721, USA
[7]Department of Ecology and Evolutionary Biology, University of Arizona, Tucson Arizona 85721, USA
[8]Department of Ecology and Evolutionary Biology and Center for Environmental Biology, University of California, Irvine, California 92697, USA
[9]Department of Geosciences, University of Arizona, Tucson, Arizona 85721, USA
[10]Department of Atmospheric Sciences, University of Arizona, Tucson, Arizona 85721, USA
[11]College of Science, University of Arizona, Tucson, Arizona 85721, USA

ABSTRACT

Basalt weathering is a key control over the global carbon cycle, though *in situ* measurements of carbon cycling are lacking. In an experimental, vegetation-free hillslope containing 330 m^3 of ground basalt scoria, we measured real-time inorganic carbon dynamics within the porous media and seepage flow. The hillslope carbon flux (0.6–5.1 mg C m^{-2} h^{-1}) matched weathering rates of natural basalt landscapes (0.4–8.8 mg C m^{-2} h^{-1}) despite lacking the expected field-based impediments to weathering. After rainfall, a decrease in CO_2 concentration ($[CO_2]$) in pore spaces into solution suggested rapid carbon sequestration but slow reactant supply. Persistent low soil $[CO_2]$ implied that diffusion limited CO_2 supply, while when sufficiently dry, reaction product concentrations limited further weathering. Strong influence of diffusion could cause spatial heterogeneity of weathering even in natural settings, implying that modeling studies need to include variable soil $[CO_2]$ to improve carbon cycling estimates associated with potential carbon sequestration methods.

INTRODUCTION

It is widely accepted that CO_2 uptake during weathering of silicate rock balances the CO_2 produced during volcanic degassing (Berner and Kothavala, 2001), yet significant uncertainty remains about the role of key controls over weathering reaction rates: climate, lithology, and erosion (Dupré et al., 2003; Kump et al., 2000). Basalt plays a large role in the regulation of atmospheric CO_2 attributable to the rapid dissolution—in comparison to other rock types—of its main constituents, such as volcanic glass, olivine, pyroxene, and plagioclase (Berg and Banwart, 2000; Gysi and Stefansson, 2012; Oelkers and Schott, 2001; Stockmann et al., 2011). In fact, CO_2 consumption associated with basalt weathering has stimulated recent geoengineering proposals to distribute basaltic minerals across landscapes as a means to draw down atmospheric CO_2 (Hartmann et al., 2013).

Measurement of watershed chemical discharges (Bouchez and Gaillardet, 2014; White, 1995) indicate basalt weathering rates orders of magnitude lower than those reported for laboratory experiments with fresh basaltic media (Gislason and Oelkers, 2003; Gislason et al., 2009; Wolff-Boenisch et al., 2006). Lower field weathering rates have been attributed to reduced reactive surface area caused by differences between laboratory and field rock matrices, including properties (in the latter) such as preferential hydrologic flow paths, lower reactive mineral-water interface in structured soils, passivation of primary mineral surfaces by secondary mineral coatings, and localized (pore-scale) variation in chemical affinity (Anbeek, 1993; Evans and Banwart, 2006; Ganor et al., 2007; Li et al., 2008; Navarre-Sitchler and Brantley, 2007). Recent thermodynamic analysis suggests that runoff and reaction product concentrations along the flow path limit weathering at field scales (Maher, 2011). Although studies have sought to reproduce rate-limiting field conditions in the laboratory, none have attempted to extend well-controlled laboratory conditions to the field scale.

In this study, we set out to observe, *in situ* and in real time, incipient weathering of basaltic porous media, without vegetation, at a field-appropriate scale. We measured pore-space CO_2 concentration ($[CO_2]$) (used to infer CO_2 removal from the atmosphere), inorganic C content in pore water, and subsequent discharge in seepage water (Fig. 1), which approximated the terrestrial carbon flux to fluvial systems. We hypothesized that a well-controlled, large-scale experiment in complex (but

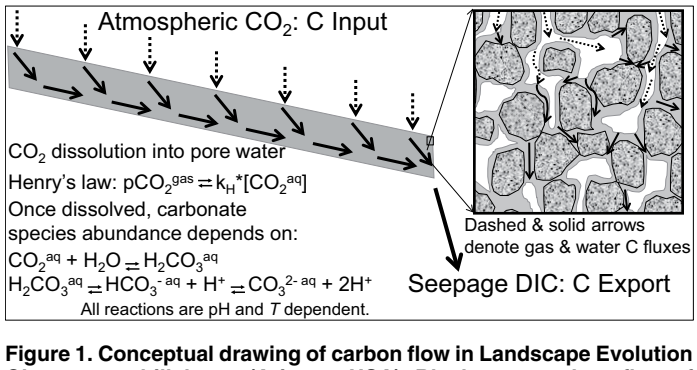

Figure 1. Conceptual drawing of carbon flow in Landscape Evolution Observatory hillslopes (Arizona, USA). Black arrows show flow of carbon through whole hillslope. Small inset depicts flow of carbon into soil pore space, where CO_2 dissolves into soil water. k_H—Henry's law constant; aq—aqueous; *T*—temperature; DIC—dissolved inorganic carbon.

*E-mail: jvanhare@email.arizona.edu

© 2017 Geological Society of America. For permission to copy, contact editing@geosociety.org.

Downloaded from https://pubs.geoscienceworld.org/gsa/geology/article-pdf/45/3/203/3549663/203.pdf
by University of Arizona user

model) terrain would help to resolve mechanisms that decrease weathering rate at larger scales. More generally, our experimental design enabled us to directly quantify the CO_2 flux from the atmosphere to river water in active weathering systems without vegetation.

METHODS SYNOPSIS

The Landscape Evolution Observatory (LEO) experimental hillslopes at Biosphere 2, near Tucson, Arizona (USA) (Gevaert et al., 2014; Pangle et al., 2015), consist of three identical convergent model landscapes (one of which was available for this experiment; Fig. DR1 in the GSA Data Repository[1]), each comprising 330 m^2 of land-atmosphere interfacial area underlain by 100 cm of loamy sand-textured basalt with porosity of 37% and bulk density of 1.5 g cm^{-3}. The resulting mineral specific surface area is 0.92 ± 0.05 m^2 g^{-1} (measured by N_2 BET [Brunauer-Emmett-Teller]; see the Data Repository), and the hillslope contains a total of ~525 Mg of ground basalt scoria with the solid phase being dominated by volcanic glass (see Table DR1 in the Data Repository).

We measured water and carbon flow from January to May of 2013 while we conducted five rain experiments on the slope. The amount of rainwater (pH = 7.1 ± 0.2, dissolved inorganic carbon [DIC] = 1.5 ± 0.9 mg L^{-1}, and calculated pCO_2 = 455 ± 130 ppm; Fig. DR2) applied by a sprinkler network was 28.7, 87.7, 22.4, 23.1, and 19.4 m^3 (or 87.0, 265.8, 67.9, 70.0, and 58.8 mm) at a rate of 12 mm hr^{-1} on day of year (DOY) 25, 49, 102, 103, and 111, respectively. Soil pore-space [CO_2], temperature, and moisture content were monitored every 15 min in 48 locations by CO_2 probes (Vaisala GMP220 [Vantaa, Finland], installed horizontally and co-located with moisture and temperature sensors and solution samplers) and in 496 locations by temperature and moisture sensors (Decagon 5TM probes [Pullman, Washington, USA]). Soil solution (496 Prenart Super Quartz pore water samplers [Frederiksberg, Denmark]) and seepage face water samples for carbonate chemistry and pH were collected when sufficient water was available. The total seepage volume was measured by a combination of in-line flow meters and tipping buckets (Pangle et al., 2015).

RESULTS

Throughout the experiment, sub-ambient [CO_2] within the soil matrix indicated sustained CO_2 consumption resulting from weathering within the basalt matrix (Fig. 2). High-resolution measurements of CO_2 in the soil gas phase during rainfall (Fig. 3) revealed a rapid [CO_2] decrease (by 200 ppm at 5 cm depth within 3 h after rainfall initiation). At greater depth, [CO_2] decreased to ~50 ppm following a 4–5 h time lag. After rainfall, soil [CO_2] recovered only slowly (~22, ~35, >50, and >50 d for 5, 20, 35, and 50 cm depth, respectively; Fig. 2). The carbon flux from the atmosphere decreased from 4 to 0.5 mg C m^{-2} h^{-1} immediately after a rain event and recovered when the soil drained (Fig. 2). From DOY 18 through 120, the average carbon flux from the atmosphere into the landscape was 3.9 ± 0.2 mg C m^{-2} h^{-1} or 31 g C d^{-1} for the whole slope. Assuming that this four-month average was representative for the whole year, this translates to ~8.5×10^{-2} kg C m^{-2} y^{-1} or ~1.2×10^{-14} mol C m^{-2} s^{-1}, where m^2 denotes the specific surface area within the soil.

DIC concentrations corroborated the low soil CO_2 measurements following rain events. Due to dilution by added rainwater, soil solution DIC concentrations decreased at 5 cm depth from 55 ± 12 to 20 ± 5 mg L^{-1} immediately following the large rain event on DOY 49 (Fig. DR6). Solution pH ranges from 8.15 to 9.97 (mean 8.78 ± 0.05, n = 308), and bicarbonate constitutes 96.9% of all DIC (carbonate ions 2.7%, and carbonic acid 0.4%). From aqueous pH, temperature, and DIC concentration, we calculated the equilibrium $CO_{2(g)}$ (g—gas) partial pressure (pCO_2) based on Henry's law and compared it to the soil CO_2 as measured by the Vaisala probes (Fig. DR3). We found a good agreement between the two data sets despite substantial scatter. The mean difference (3.7 ± 4.8 ppm) was not statistically different from zero (two-tailed t_{276}= 1.5, p = 0.13; Fig. DR3 inset).

DIC concentration in seepage water was comparable to that measured in slope pore water prior to the large rain events. Immediately following the DOY 49 rain event, seepage water DIC concentrations decreased by a factor of two to three (Fig. DR4a). Subsequent rain events, with a lower water volume, resulted in smaller decreases in DIC concentration and smaller seepage volumes (Fig. DR4b). The maximum amount of carbon

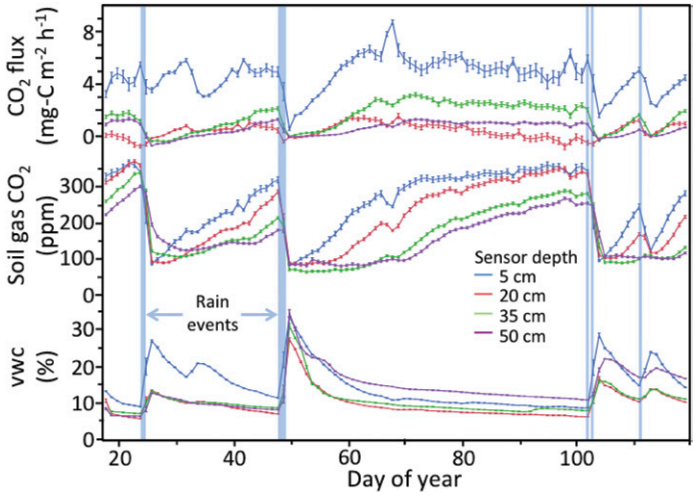

Figure 2. Landscape soil CO_2 and moisture content responses to rainfall pulses at the Landscape Evolution Observatory (Arizona, USA). Trends of volumetric water content (VWC, bottom), CO_2 concentration (middle), and CO_2 flux (top) across experimental period demonstrate rapid response to rainfall events (denoted by vertical blue bars). Data were averaged daily across the slope for each depth and variable (error bars denote 95% CI).

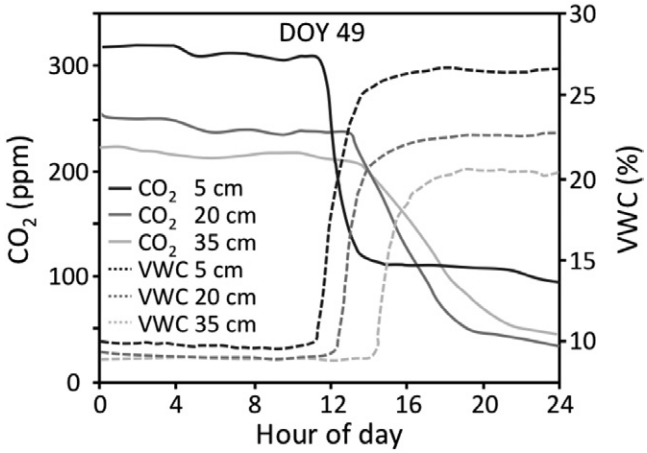

Figure 3. Rapid response of soil moisture and gas phase CO_2 concentration at one profile location to rainfall event on day of year (DOY) 49 at the Landscape Evolution Observatory (Arizona, USA). Lines represent running mean values of sensors at depths of 5, 20, and 35 cm. VWC—volumetric water content.

[1]GSA Data Repository item 2017053, methods; full description and visualization (Figure DR1) of the Landscape Evolution Experiment; carbon within the rain, slope and seepage water (Figure DR2); measured and calculated soil gas CO_2 concentrations (Figure DR3); carbon export seepage (Figure DR4); measured and laboratory weathering rate based carbon uptake rates (Figure DR5); seepage cation and anion concentrations (Figure DR6), chemical composition of basalt substrates (Table DR1); global carbon uptake rates (Table DR2); and saturation states of secondary minerals within the slope (Table DR3), is available online at www.geosociety.org/datarepository/2017 or on request from editing@geosociety.org.

Downloaded from https://pubs.geoscienceworld.org/gsa/geology/article-pdf/45/3/203/3549663/203.pdf
by University of Arizona user

exported from the whole landscape in 15 min was 23 g. In 10 d after the DOY 49 rain event, the total amount of carbon exported from the whole slope was ~5 kg (Fig. 4).

DISCUSSION

Observed mass balance and fluxes of inorganic carbon among soil gas, pore water, and saturated zone seepage of the LEO landscape demonstrated the rapid CO_2 sequestration potential of basalt. CO_2 fluxes were comparable to exchange rates in basalts as calculated from integrated riverine measurements (Dessert et al., 2003; Li et al., 2016) (Table DR2) and surface area (Navarre-Sitchler and Brantley, 2007), but were orders of magnitude slower than laboratory weathering rates.

To address the apparently low weathering rates in the LEO, we calculated how much of the actual basalt surface area reacted with the solution based on laboratory dissolution rates. We assumed that the main reacting phase was basaltic glass, which encases most mineral phases (Dontsova et al., 2014), and the main controlling factor pH. We therefore based our calculation on laboratory dissolution rates of basaltic glass at 20–25 °C and pH 8.3–9.0 (Stockmann et al., 2011), conditions akin to those within the LEO slope. Our calculation indicated that only 0.036%–0.074% of the total basalt surface area was active in generating observed DIC export (Fig. DR5). An independent estimate of surface area was obtained from Na exported with seepage (570 mol over 105 d) and chemical composition of basaltic glass (Table DR1). Na was only released by basalt weathering with no Na-containing secondary phases precipitating (Eiriksdottir et al., 2013), as predicted by geochemical modeling (Pohlmann et al., 2016). We calculated that 126–131 kg of basalt produced Na ions during weathering, or 0.043% of the total slope basalt mass (524.7 Mg). Both calculations indicate that only a small percentage of the slope was active if surface weathering rates were comparable to laboratory rates.

Several lines of evidence suggest that we can rule out preferential flow paths, such as finger flow, and secondary mineral precipitation as significant controls on the low apparent weathering rate. During construction, the LEO was packed to a relatively isotropic and homogeneous distribution of material and bulk density. After the large precipitation event (DOY 49; Gevaert et al., 2014), some heterogeneity did develop and caused rapid saturation of the landscape. However, the relative homogeneity of soil moisture at a given depth with time (Fig. 2) indicated that wetting of the slope was nearly uniform (Gevaert et al., 2014). The secondary mineral phase most likely to have precipitated within the LEO was the poorly crystalline aluminosilicate, allophane (Pohlmann et al., 2016). Based on the number of moles of Na exported and the stoichiometry, molar mass, particle size, and specific surface area of allophane (Parfitt, 2009; Wada et al., 1988), we calculated that a monolayer of allophane at most would cover ~0.5% of the total basalt surface area within the slope (~2.5×10^9 m^2). Cation export by the seepage solution suggested that other Fe-, Mn-, Ca-, and Mg-containing phases must have precipitated within the slope (Fig. DR6; Pohlmann et al., 2016). However, based on our allophane monolayer calculation and relatively low surface affinity of other secondary mineral phases (Stockmann et al., 2011), we consider the likelihood very low that any phase would have greatly diminished the reactive surface area.

Substantial runoff could represent another potential cause for decrease in apparent surface area, because runoff water never enters the slope to react with the material. Strong fluid disequilibrium due to runoff (resulting in lower reactant concentrations; Maher, 2011) was observed once in the seepage flow, when after the DOY 49 rainfall event the DIC concentration decreased substantially (Fig. DR4). Recovery of the DIC after the rain event was within days, suggesting that equilibrium between the fluid and solids was reached quickly. The lower DIC (Fig. DR4) and ion concentrations (Fig. DR6) over time suggest that either the equilibrium path or time length increased with age of the slope or that the effective [CO_2] decreased over time (see Maher, 2011, her figure 4B).

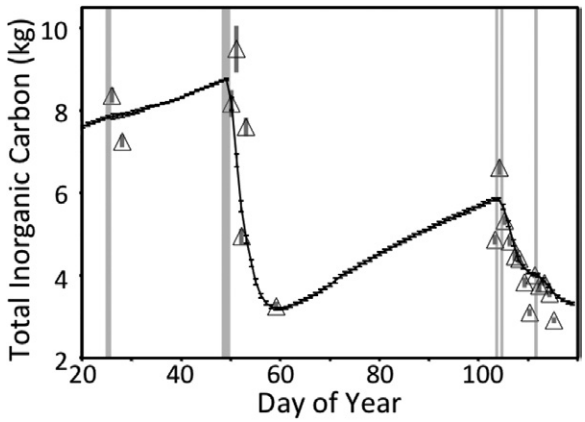

Figure 4. Carbon mass balance of the Landscape Evolution Observatory (Arizona, USA) landscape. Measured within-slope total dissolved inorganic carbon (DIC, triangles) is matched by predicted slope total DIC (black line) based on carbon added to soil from atmosphere and exported from soil in seepage solution, suggesting that carbon mass balance is well conserved. Vertical gray bars denote the 95% confidence interval of the mean carbon content within the slope based on DIC and moisture content variability.

Pore solution DIC and gas phase [CO_2] provided direct evidence for limitation of weathering reactions by diffusion of CO_2 from the atmosphere to soil pore spaces in our experimental, field-scale basalt landscape without vegetation. Maher (2011) demonstrated using reactive transport calculations (CrunchFlow software) that in unsaturated conditions, water content and [CO_2] both control the final equilibrium solute concentration and scale (length or time). In her calculations, [CO_2] was more important than water content with respect to overall weathering rate, and increased [CO_2] and decreased water content led to higher equilibrium concentrations and longer equilibration times. These calculations however, were based on the assumption of a constant [CO_2] in the unsaturated zone. Our measurements suggest that this assumption is not applicable for nearly abiotic systems and that the disequilibrium between atmospheric and soil CO_2 can be large and quick to develop after a rainfall event (Fig. 3), indicative of a faster gas-to-solution transfer rate than the modeled carbon flux (Fig. 2, top). Low soil [CO_2] can lead to cascading effects by reducing the final solute equilibrium concentration and equilibrium path length or time (Maher, 2011). For several weeks after the rainfall event, soil gaseous [CO_2] was in equilibrium with the soil solution (Fig. DR3) but not with the atmosphere. The disequilibrium between atmospheric and soil gas [CO_2] strongly suggests that transport of gaseous CO_2 from the atmosphere could not match the uptake of CO_2 into the soil solution. We interpreted these results to imply that soil gas diffusion limited weathering reactions by not supplying ample reactant (CO_2). Once the water content decreased enough for the soil [CO_2] to equilibrate with the atmosphere (22, 40, and >50 d at 5, 20, and >35 cm depth, respectively, in the LEO; Fig. 2), weathering most likely was limited due to the soil solution saturation with respect to the reaction products due to evaporation and/or sufficient reaction time.

Most soils are not alkaline and have ample vegetation, which produces high [CO_2] through root and soil organic matter respiration. Although rare, low soil [CO_2] has been found in alkaline desert environments in the Mojave Desert, southwest USA (Wohlfahrt et al., 2008), and in Antarctica (Shanhun et al., 2012). Furthermore, CO_2 uptake has been found in ultramafic mine tailings (Pronost et al., 2012; Harrison et al., 2013) and can partially offset carbon emissions by the mining operation. In these environments, direct CO_2 uptake from the atmosphere can lead to carbon sequestration, however likely not enough to offset human carbon emissions. Diffusion limitation to weathering would reduce the sequestration

Downloaded from https://pubs.geoscienceworld.org/gsa/geology/article-pdf/45/3/203/3549663/203.pdf
by University of Arizona user

benefit of tailings and vegetation-free basalt flows, which have lower weathering rates than vegetated flows (Moulton and Berner, 1998). Furthermore, we recommend that modeling efforts take into account variable soil [CO_2] in unsaturated zones and a mechanism of reducing weathering rate through low diffusion rates in soils. This likely will also have implications for soils with sparse vegetation, where if diffusion is slow, strong spatial variability in soil [CO_2] and weathering rates could be maintained.

Lastly, our landscape carbon balance appeared to be well closed (Fig. 4). Total carbon within the slope was matched by a simple prediction of initial carbon (based on pore water DIC measurements and water content) with carbon added from the atmosphere and subtracted by export in seepage water. Our capability to calculate mass balance carbon dynamics within the LEO model landscape (Fig. 4) provides robust experimental evidence that riverine export of carbon from abiotic watersheds indeed represents carbon uptake at the landscape scale.

ACKNOWLEDGMENTS

We acknowledge support from the Philecology Foundation (Fort Worth, Texas, USA) and its founder, Mr. Edward Bass. Additional support was provided by the Water, Environmental, and Energy Solutions (WEES) initiative at the University of Arizona, and by the Office of the Vice President of Research at the University of Arizona. The use of firm, trade, and brand names does not constitute endorsement by the authors or their employers. The paper benefited greatly from thoughtful comments by M. Winnick, M. Schultz, and anonymous reviewers.

REFERENCES CITED

Anbeek, C., 1993, The effect of natural weathering on dissolution rates: Geochimica et Cosmochimica Acta, v. 57, p. 4963–4975, doi:10.1016/S0016-7037(05)80002-X.

Berg, A., and Banwart, S.A., 2000, Carbon dioxide mediated dissolution of Ca-feldspar: Implications for silicate weathering: Chemical Geology, v. 163, p. 25–42, doi:10.1016/S0009-2541(99)00132-1.

Berner, R.A., and Kothavala, Z., 2001, GEOCARB III: A revised model of atmospheric CO_2 over Phanerozoic time: American Journal of Science, v. 301, p. 182–204, doi:10.2475/ajs.301.2.182.

Bouchez, J., and Gaillardet, J., 2014, How accurate are rivers as gauges of chemical denudation of the Earth surface?: Geology, v. 42, p. 171–174, doi:10.1130/G34934.1.

Dessert, C., Dupre, B., Gaillardet, J., Francois, L.M., and Allegre, C.J., 2003, Basalt weathering laws and the impact of basalt weathering on the global carbon cycle: Chemical Geology, v. 202, p. 257–273, doi:10.1016/j.chemgeo.2002.10.001.

Dontsova, K., Zaharescu, D., Henderson, W., Verghese, S., Perdrial, N., Hunt, E., and Chorover, J., 2014, Impact of organic carbon on weathering and chemical denudation of granular basalt: Geochimica et Cosmochimica Acta, v. 139, p. 508–526, doi:10.1016/j.gca.2014.05.010.

Dupré, B., Dessert, C., Oliva, P., Godderis, Y., Viers, J., Francois, L., Millot, R., and Gaillardet, J., 2003, Rivers, chemical weathering and Earth's climate: Comptes Rendus Geoscience, v. 335, p. 1141–1160, doi:10.1016/j.crte.2003.09.015.

Eiriksdottir, E.S., Gislason, S.R., and Oelkers, E.H., 2013, Does temperature or runoff control the feedback between chemical denudation and climate? Insights from NE Iceland: Geochimica et Cosmochimica Acta, v. 107, p. 65–81, doi:10.1016/j.gca.2012.12.034.

Evans, K.A., and Banwart, S.A., 2006, Rate controls on the chemical weathering of natural polymineralic material: I. Dissolution behaviour of polymineralic assemblages determined using batch and unsaturated column experiments: Applied Geochemistry, v. 21, p. 352–376, doi:10.1016/j.apgeochem.2005.10.001.

Ganor, J., Lu, P., Zheng, Z.P., and Zhu, C., 2007, Bridging the gap between laboratory measurements and field estimations of silicate weathering using simple calculations: Environmental Geology, v. 53, p. 599–610, doi:10.1007/s00254-007-0675-0.

Gevaert, A.I., et al., 2014, Hillslope-scale experiment demonstrates the role of convergence during two-step saturation: Hydrology and Earth System Sciences, v. 18, p. 3681–3692, doi:10.5194/hess-18-3681-2014.

Gislason, S.R., and Oelkers, E.H., 2003, Mechanism, rates, and consequences of basaltic glass dissolution: II. An experimental study of the dissolution rates of basaltic glass as a function of pH and temperature: Geochimica et Cosmochimica Acta, v. 67, p. 3817–3832, doi:10.1016/S0016-7037(03)00176-5.

Gislason, S.R., et al., 2009, Direct evidence of the feedback between climate and weathering: Earth and Planetary Science Letters, v. 277, p. 213–222, doi:10.1016/j.epsl.2008.10.018.

Gysi, A.P., and Stefansson, A., 2012, CO_2-water-basalt interaction: Low temperature experiments and implications for CO_2 sequestration into basalts: Geochimica et Cosmochimica Acta, v. 81, p. 129–152, doi:10.1016/j.gca.2011.12.012.

Harrison, A.L., Power, I.M., and Dipple, J.M., 2013, Accelerated carbonation of brucite in mine tailings for carbon sequestration: Environmental Science & Technology, v. 47, p. 126–134, doi:10.1021/es3012854.

Hartmann, J., West, A.J., Renforth, P., Kohler, P., De La Rocha, C.L., Wolf-Gladrow, D.A., Durr, H.H., and Scheffran, J., 2013, Enhanced chemical weathering as a geoengineering strategy to reduce atmospheric carbon dioxide, supply nutrients, and mitigate ocean acidification: Reviews of Geophysics, v. 51, p. 113–149, doi:10.1002/rog.20004.

Kump, L.R., Brantley, S.L., and Arthur, M.A., 2000, Chemical, weathering, atmospheric CO_2, and climate: Annual Review of Earth and Planetary Sciences, v. 28, p. 611–667, doi:10.1146/annurev.earth.28.1.611.

Li, G.J., et al., 2016, Temperature dependence of basalt weathering: Earth and Planetary Science Letters, v. 443, p. 59–69, doi:10.1016/j.epsl.2016.03.015.

Li, L., Steefel, C.I., and Yang, L., 2008, Scale dependence of mineral dissolution rates within single pores and fractures: Geochimica et Cosmochimica Acta, v. 72, p. 360–377, doi:10.1016/j.gca.2007.10.027.

Maher, K., 2011, The role of fluid residence time and topographic scales in determining chemical fluxes from landscapes: Earth and Planetary Science Letters, v. 312, p. 48–58, doi:10.1016/j.epsl.2011.09.040.

Moulton, K.L., and Berner, R.A., 1998, Quantification of the effect of plants on weathering: Studies in Iceland: Geology, v. 26, p. 895–898, doi:10.1130/0091-7613(1998)026<0895:QOTEOP>2.3.CO;2.

Navarre-Sitchler, A., and Brantley, S., 2007, Basalt weathering across scales: Earth and Planetary Science Letters, v. 261, p. 321–334, doi:10.1016/j.epsl.2007.07.010.

Oelkers, E.H., and Schott, J., 2001, An experimental study of enstatite dissolution rates as a function of pH, temperature, and aqueous Mg and Si concentration, and the mechanism of pyroxene/pyroxenoid dissolution: Geochimica et Cosmochimica Acta, v. 65, p. 1219–1231, doi:10.1016/S0016-7037(00)00564-0.

Pangle, L.A., et al., 2015, The Landscape Evolution Observatory: A large-scale controllable infrastructure to study coupled Earth-surface processes: Geomorphology, v. 244, p. 190–203, doi:10.1016/j.geomorph.2015.01.020.

Parfitt, R.L., 2009, Allophane and imogolite: Role in soil biogeochemical processes: Clay Minerals, v. 44, p. 135–155, doi:10.1180/claymin.2009.044.1.135.

Pohlmann, M.K., Dontsova, K., Root, R., Ruiz, J., Troch, P.A., and Chorover, J., 2016, Pore water chemistry reveals gradients in mineral transformation across a model basaltic hillslope: Geochemistry Geophysics Geosystems, v. 17, p. 2054–2069, doi:10.1002/2016GC006270.

Pronost, J., et al., 2012, CO_2-depleted warm air venting from chrysotile milling waste (Thetford Mines, Canada): Evidence for in-situ carbon capture from the atmosphere: Geology, v. 40, p. 275–278, doi:10.1130/G32583.1.

Shanhun, F.I., Almond, P.C., Clough, T.J., and Smith, C.M.S., 2012, Abiotic processes dominate CO_2 fluxes in Antarctic soils: Soil Biology and Biochemistry, v. 53, p. 99–111, doi:10.1016/j.soilbio.2012.04.027.

Stockmann, G.J., Wolff-Boenisch, D., Gislason, S.R., and Oelkers, E.H., 2011, Do carbonate precipitates affect dissolution kinetics? 1: Basaltic glass: Chemical Geology, v. 284, p. 306–316, doi:10.1016/j.chemgeo.2011.03.010.

Wada, K., Wilson, M., Kakuto, Y., and Wada, S.I., 1988, Synthesis and characterization of a hollow spherical form of monolayer aluminosilicate: Clays and Clay Minerals, v. 36, p. 11–18, doi:10.1346/CCMN.1988.0360102.

White, A.F., 1995, Chemical weathering rates of silicate minerals in soils, *in* White, A., and Brantley, S., eds., Chemical Weathering Rates of Silicate Minerals: Washington, D.C., Mineralogical Society of America, Reviews in Mineralogy, v. 31, p. 407–458.

Wohlfahrt, G., Fenstermaker, L.F., and Arnone, J.A., 2008, Large annual net ecosystem CO_2 uptake of a Mojave desert ecosystem: Global Change Biology, v. 14, p. 1475–1487, doi:10.1111/j.1365-2486.2008.01593.x.

Wolff-Boenisch, D., Gislason, S.R., and Oelkers, E.H., 2006, The effect of crystallinity on dissolution rates and CO_2 consumption capacity of silicates: Geochimica et Cosmochimica Acta, v. 70, p. 858–870, doi:10.1016/j.gca.2005.10.016.

Manuscript received 1 September 2016
Revised manuscript received 8 November 2016
Manuscript accepted 9 November 2016

Printed in USA

Downloaded from https://pubs.geoscienceworld.org/gsa/geology/article-pdf/45/3/203/3549663/203.pdf
by University of Arizona user